

# Modeling of Weakly Conducting Thin Sheets in the Discontinuous Galerkin Method for Shielding Effectiveness Evaluation

M. Boubekur<sup>1</sup>, A. Kameni<sup>1</sup>, A. Modave<sup>2</sup>, L. Bernard<sup>1</sup>, and L. Pichon<sup>1</sup>

<sup>1</sup>Laboratoire de Génie Electrique de Paris, UMR 8507 CNRS, SUPELEC, Université Paris-Sud  
Université Pierre et Marie Curie, 11 rue Joliot-Curie, 91192 Gif-sur-Yvette, France  
Mohamed.boubekur@lgep.supelec.fr, abelin.kameni@lgep.supelec.fr, laurent.bernard@lgep.supelec.fr,  
lionel.pichon@lgep.supelec.fr

<sup>2</sup>Université de Liège, Department of Electrical Engineering and Computer Science, Applied and  
Computational Electromagnetics, Liège 4000, Belgium  
a.modave@ulg.ac.be

**Abstract** – This paper presents a modeling of weakly conducting thin sheets in the time domain discontinuous Galerkin method. This interface condition is used to avoid the mesh of resistive sheets in order to evaluate the shielding effectiveness in high frequency electromagnetic compatibility problems. This condition is valid when the thickness of the sheet is smaller than the skin depth. This approach is validated by a comparison with an analytical solution. A 1D two sheets example, 2D and 3D cavities are treated to illustrate the efficiency of the condition.

**Index Terms** – Discontinuous Galerkin, resistive sheet, and shielding effectiveness.

## I. INTRODUCTION

The accurate evaluation of the shielding effectiveness of enclosures of complex shapes is a crucial issue in many electromagnetic compatibility (EMC) problems. It requires adequate numerical approaches. The ability to model features that are small relative to the cell size is often important in electromagnetic simulations. This may lead to subsequent increase in memory and execution time due to a refined mesh around small details of the geometry. This is particularly true for thin sheets, which may involve a mesh of bad quality.

In order to avoid the spatial discretization of thin sheets, different interface conditions have

been proposed. In the frequency domain, analytical solutions [1, 2] can be included in a three dimensional model [3]. Many papers have been devoted to extend the approach in the time domain using an inverse Fourier or Laplace transform combined to a convolution product with the FDTD method [4-6]. Nevertheless, the stair casing error present in the FDTD method may affect significantly the numerical results.

The discontinuous Galerkin (DG) method is a powerful approach for solving time dependent problems. It is based on the local resolution of the equations in each cell and uses flux terms to connect adjacent elements [7-9]. It has the advantage of the unstructured mesh and high spatial order unlike the conventional FDTD. Such a high level spatial scheme can reduce the dispersive error induced by the low level of the spatial approximation in the FDTD.

Composite materials become widely used in aerospace and aircraft industries. They are generally composed by a resin matrix reinforced by conducting fibres [10, 11]. These materials offer low weight but are not as electrically conductive as metallic ones. So they have a significant impact on the electromagnetic behaviour of the enclosures. The effect of such a low conductivity on the envelope resonances needs to be studied.

In [12] a resistive sheet was proposed for a DG method based on hexahedral elements. It showed its advantages in terms of accuracy and

memory storage compared with the FDTD method but suffers from the use of cubic cells.

In this paper a specific interface condition is proposed to replace a thin resistive cell in a DG method based on an unstructured mesh. The formalism is developed in the general 3D case, it is then implemented for simplex elements in 2D (triangles) and 3D (tetrahedral). It allows to take into account conductors with a thickness smaller than the skin depth. This method is implemented in a DG module of GMSH [13].

## II. PROBLEM FORMULATION

The Maxwell's equations are solved in the time domain as,

$$\begin{cases} \varepsilon \partial_t \vec{E} - \nabla \times \vec{H} = -\vec{J} \\ \mu \partial_t \vec{H} + \nabla \times \vec{E} = 0 \end{cases}, \quad (1)$$

where  $\varepsilon$  is the permittivity of the medium and  $\mu$  its permeability. The current density of the conductive medium is such as  $\vec{J} = \sigma \vec{E}$ , with  $\sigma$  is the conductivity.

For the computational applications, the fields are discretized on a mesh made of triangular or tetrahedral elements, with first-order basis functions. The time-stepping is performed with the leapfrog scheme. The numerical scheme is based on the variational formulation of equation (1) given by, in each tetrahedral element  $T$ ,

$$\begin{cases} \int_T \varepsilon \frac{\vec{E}^{n+1} - \vec{E}^n}{\Delta t} \cdot \vec{\Phi} = [\int_T \vec{H}^{n+\frac{1}{2}} \cdot \nabla \times \vec{\Phi} \\ + \int_{\partial T} (\vec{n} \times \vec{H})^{\text{num}, n+\frac{1}{2}} \cdot \vec{\Phi} - \int_T \sigma \vec{E}^n \cdot \vec{\Phi}] \\ \int_T \mu \frac{\vec{H}^{n+\frac{1}{2}} - \vec{H}^{n-\frac{1}{2}}}{\Delta t} \cdot \vec{\Phi} = -[\int_T \vec{E}^n \cdot \nabla \times \vec{\Phi} \\ + \int_{\partial T} (\vec{n} \times \vec{E})^{\text{num}, n} \cdot \vec{\Phi}] \end{cases}, \quad (2)$$

where  $(\vec{n} \times \vec{E})^{\text{num}}$  and  $(\vec{n} \times \vec{H})^{\text{num}}$  are the numerical flux that must be evaluated with a particular discretization. There are generally two choices, which make the scheme dissipative or dispersive,

$$\begin{cases} (\vec{n} \times \vec{H})^{\text{num}, n+\frac{1}{2}} = \vec{n} \times \frac{\{Z\vec{H}^{n+\frac{1}{2}}\}}{\{Z\}} - \alpha \left( \vec{n} \times \frac{(\vec{n} \times \{\vec{E}^n\})}{\{Z\}} \right) \\ (\vec{n} \times \vec{E})^{\text{num}, n} = \vec{n} \times \frac{\{Y\vec{E}^n\}}{\{Y\}} + \alpha \left( \vec{n} \times \frac{(\vec{n} \times \{\vec{H}^{n-\frac{1}{2}}\})}{\{Y\}} \right) \end{cases}, \quad (3)$$

where  $\vec{n}$  the outward normal,  $Z = 1/Y = \sqrt{\mu/\varepsilon}$ ,  $\{u\} = \frac{u^+ - u^-}{2}$  and  $\{u\} = \frac{u^+ + u^-}{2}$ . The subscript “-” denotes the values for fields in the current element, while “+” is for the adjacent element. For  $\alpha = 0$ , centred flux are obtained and the numerical scheme is dispersive [14]. For  $\alpha = 1$ , upwind flux are obtained and the numerical scheme is dissipative [8]. In this work, upwind fluxes are used. For expensive reference simulations (when the sheet is meshed and 3D cavity), an implicit Runge-Kutta scheme that permits a large time step is considered.

## III. CONSTRUCTION OF THE INTERFACE CONDITION

The electromagnetic field equations in the sheet are considered in 1D and in the frequency domain,

$$\begin{cases} \partial_x E_y = -j\omega\mu H_z \\ \partial_x H_z = -(\sigma + j\omega\varepsilon)E_y \end{cases}, \quad (4)$$

where  $\varepsilon$ ,  $\mu$ , and  $\sigma$  are respectively the permittivity, the permeability, and the conductivity of the sheet (Fig. 1).

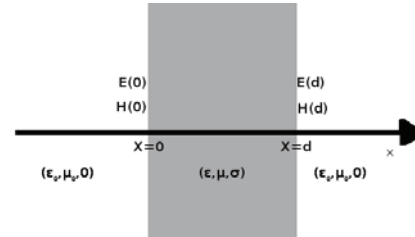


Fig. 1. Resistive sheet.

So the intrinsic impedance of the sheet is,

$$\eta = \sqrt{\frac{j\omega\mu}{\sigma + j\omega\varepsilon}}, \quad (5)$$

and the planar propagation constant is,

$$\gamma = \sqrt{j\omega\mu(\sigma + j\omega\varepsilon)}. \quad (6)$$

For low frequency, the impedance and the propagation constant can be written as,

$$\begin{cases} \eta = \sqrt{\frac{j\omega\mu}{\sigma}} \\ \gamma = \sqrt{j\omega\mu\sigma} \end{cases}. \quad (7)$$

Using the analytical 1D solution [5], the electromagnetic fields on the two sides of the shield are connected by,

$$\begin{pmatrix} H_z(\omega, 0) \\ H_z(\omega, d) \end{pmatrix} = M \begin{pmatrix} E_y(\omega, 0) \\ E_y(\omega, d) \end{pmatrix} \quad (8)$$

where  $M$  is the admittance matrix,

$$M = \begin{pmatrix} y_1(\omega) & -y_2(\omega) \\ y_2(\omega) & -y_1(\omega) \end{pmatrix}. \quad (9)$$

$y_{11}$  and  $y_{21}$  have the following expression,

$$\begin{aligned} y_1(\omega) &= -(\eta \tanh(\gamma d))^{-1} \\ y_2(\omega) &= -(\eta \sinh(\gamma d))^{-1}. \end{aligned} \quad (10)$$

The asymptotic behaviour of  $y_{11}$  and  $y_{21}$ , when  $\omega \rightarrow 0$ ,

$$\begin{aligned} y_1 &\sim y_1^{LF} = -\frac{i}{\omega\mu d} \frac{\sigma d}{3} + O(\omega) \\ y_2 &\sim y_2^{LF} = -\frac{i}{\omega\mu d} + \frac{\sigma d}{6} + O(\omega). \end{aligned} \quad (11)$$

For the low frequencies,  $(y_2 - y_1) \approx \frac{\sigma d}{2}$ . The error of this approximation depends on  $\gamma d$ . The real and imaginary parts of  $\gamma d$  are equal to  $\frac{d}{\delta}$ , where  $\delta = \sqrt{\frac{2}{\mu\sigma\omega}}$  is the skin depth. So the error of the approximation is determined by the rate  $\frac{d}{\delta}$ . For our problem, we choose  $\frac{d}{\delta} \leq 1$ . In the worst case (i.e.,  $d = \delta$ ), the error on  $(y_2 - y_1)$  is then approximately 3 %.

The continuity of the electric field is supposed, and a simplified relation is deduced,

$$\begin{cases} E_y(\omega, 0) = E_y(\omega, d) \\ H_z(\omega, d) - H_z(\omega, 0) = \sigma d \frac{E_y(\omega, 0) + E_y(\omega, d)}{2}. \end{cases} \quad (12)$$

For the time domain application, due to the linearity of the relation, it stays unchanged,

$$\begin{cases} E_y(t, 0) = E_y(t, d) \\ H_z(t, d) - H_z(t, 0) = \sigma d \frac{E_y(t, 0) + E_y(t, d)}{2}. \end{cases} \quad (13)$$

The relation of equation (12) can be formulated with the tangential components of the fields,

$$\begin{cases} \vec{n} \times \vec{E}^+ = \vec{n} \times \vec{E}^- \\ \vec{n} \times \vec{H}^+ - \vec{n} \times \vec{H}^- = Y_s \vec{n} \times \vec{n} \times \frac{(\vec{E}^- + \vec{E}^+)}{2}, \end{cases} \quad (14)$$

where  $\vec{n}$  is the outward unit normal of the  $(\vec{E}^-, \vec{H}^-)$  element and  $Y_s = \sigma d$ . The propagation of a plane wave with normal incidence is considered from “-” incident medium to “+”. The resulting flux terms for the proposed interface condition are obtained using equation (13) and flux term in equation (3) with  $\alpha = 0$ .  $(\vec{n} \times \vec{E})^{\text{num}}$  stays unchanged relative to equation (3) thanks to the continuity of the electric field. To define  $(\vec{n} \times \vec{H})^{\text{num}}$ ,  $\vec{n} \times \frac{\{Z\vec{H}\}}{\{Z\}}$  is replaced by  $\vec{n} \times \vec{H}^+$  computed using equation (14),

$$\begin{cases} (\vec{n} \times \vec{H})^{\text{num}} = \vec{n} \times \vec{H}^- + Y_s \vec{n} \times \vec{n} \times \{\vec{E}\} \\ (\vec{n} \times \vec{E})^{\text{num}} = \vec{n} \times \frac{\{Y\vec{E}\}}{\{Y\}} \end{cases}. \quad (15)$$

## IV. 1D TEST EXAMPLE

### A. Validation test

To validate this condition, we consider  $\vec{E} = (0, 0, E_z)$  and  $\vec{H} = (0, H_y, 0)$ , and two domains separated by a sheet of 1 mm thickness (Fig. 1). This sheet is illuminated by a planar cosine pulse with frequency  $f = 100$  MHz. The transmitted and reflected fields are computed for  $\sigma \in [1, 500]$  S/m. The minimal skin depth is 2.25 mm. Figure 2 illustrates the comparison between the transmitted field of the computed solution and the analytical solution, which is calculated in the frequency domain. The difference between the analytical and computed solution is negligible.

For the same example, the frequency is varied from 100 MHz to 1000 MHz, for conductivity  $\sigma = 100$  S/m. The shielding effectiveness for the electric field is defined by the following expression,

$$SE_E = 20 \log_{10} \left| \frac{\vec{E}_i}{\vec{E}_t} \right|, \quad (15)$$

where  $\vec{E}_i$  is the incident electric field and  $\vec{E}_t$  is the transmitted electric field.

The error on the shielding effectiveness of the sheet between analytical and computed solution remains less than 1%. These examples validate the interface condition when the skin depth is larger than the thickness of the sheet.

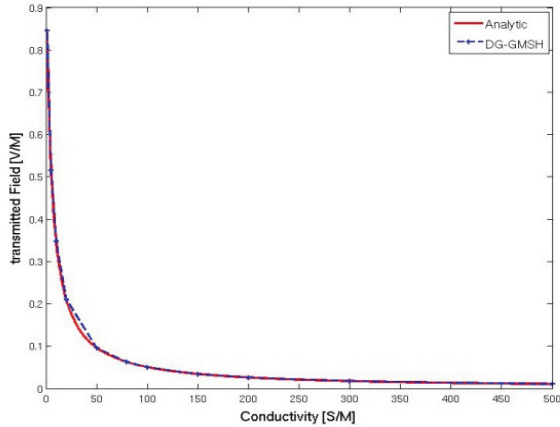


Fig. 2. Transmitted field.

**B. Double sheets**

The incident electromagnetic field is similar to the first example. Three domains separated by two sheets of 1 mm thickness and conductivity  $\sigma = 50$  S/m are considered. The distance between the two sheets is 10 cm (Fig. 3). The incident field is a Gaussian pulse  $E_z = e^{-a(t-t_0)^2}$  centered at  $t_0 = 5.10^{-9}$  s, with the parameter  $a = \frac{9.10^{16} \log_{10}(100)}{(0.75)^2} s^{-2}$ . In this example, three solutions are compared (Fig. 4). The first one corresponds to the situation where the sheet is meshed. This problem is solved with DG method. The second one is solved with finite integration technique (FIT) [15]. The third one corresponds to the interface condition and is solved with DG method. A good agreement is obtained with the interface condition; the computational time is reduced by a factor of 10. This is due to the fact that in the case where the sheet is meshed a great number of elements are required. Moreover, an implicit scheme is needed to avoid a reduced time step. The FIT method solution has the same behaviour but the maximum value is less important than for the other solutions.

**V. 2D CAVITY**

An illustration of this DG scheme is presented in a 2D case with the interface condition. Let us consider a cavity whose dimensions are 50 cm  $\times$  40 cm. A 10 cm aperture is located on the front side. The thickness of the wall is 1 mm (Fig. 5). The incident field is a product between cosine and

a sinus cardinal.  $E_z = \text{sinc}(w_r(t - t_0)) \cos(w_c(t - t_0))$  with  $w_r = 300$  MHz and  $w_c = 700$  MHz. This field is centered at  $t_0 = 5.10^{-8}$  s, and excites a large frequency band  $f \in [400, 1000]$  MHz.

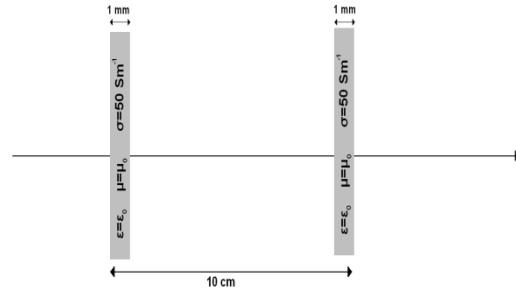


Fig. 3. Double conductive sheet.

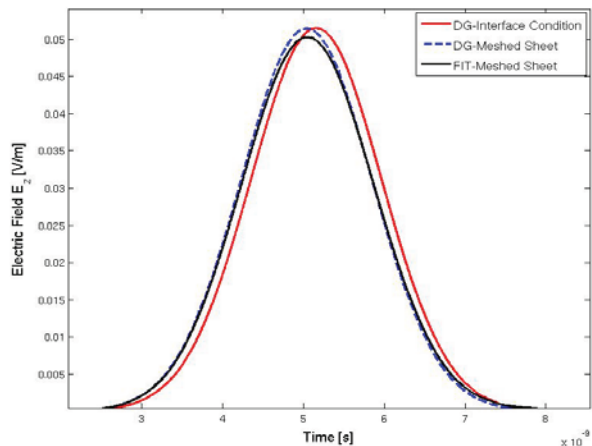


Fig. 4. Transmitted field in the midpoint between the sheets.

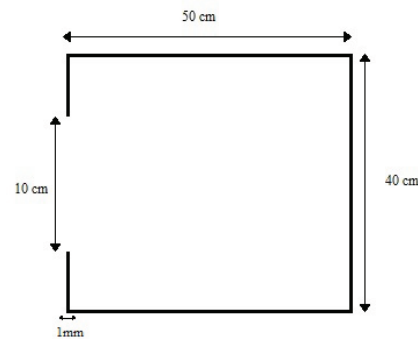


Fig. 5. 2D cavity.

A fast Fourier transform (FFT) is applied to the total field at the center of the cavity. Different cases are considered. The perfect electric conductor (PEC) case is computed with DG

method and FIT method. The cases of finite conductivity values are computed with the interface condition with DG method.

In Fig. 6 the shielding effectiveness is plotted at the center of the cavity for the different cases. The results obtained with the PEC interface condition in DG method (red) is close to that obtained with FIT (blue). For finite values of conductivity  $\sigma = 100$  S/m (green) and  $\sigma = 10$  S/m (black), it can be noted that the resonance peaks are attenuated due to the conductivity. This behaviour is in accordance to that observed in a composite shield studied in the frequency domain [16]. In Fig. 7 the total electric field is compared at the center of the cavity when it is illuminated by the Gaussian pulse used in the 1D example. The different cases considered are the PEC wall in DG (red) and FIT (blue), the conductive wall with  $\sigma = 10$  S/m (purple) and  $\sigma = 50$  S/m (black) in DG with interface condition.

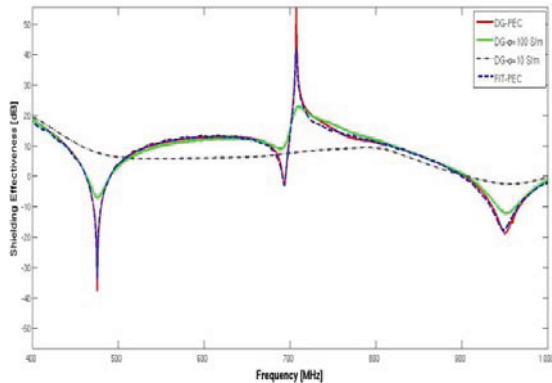


Fig. 6. Shielding effectiveness in the center of the cavity.

For the PEC wall, the field penetrates only by the aperture. In case of resistive walls the fields propagate through the walls and aperture. So the fields inside the cavity decrease faster with time for low conductivities.

### VI. 3D CAVITY

Let us consider 3D cavity (Fig. 8), whose dimensions are  $a = 300$  mm,  $b = 120$  mm,  $d = 300$  mm,  $l = 100$  mm,  $w = 5$  mm and  $t = 1$  mm[17]. This cavity is illuminated by an incident Gaussian pulse  $E_z = e^{-a(t-t_0)^2}$  centered at  $t_0 = 1,5 \cdot 10^{-9}$  s, with the parameter

$a = \frac{(11 \cdot 10^9)^2}{4 \log_{10}(100)} s^{-2}$ . The electric field is computed at the center of the cavity. Different cases of conductivity of the sheet are compared,  $\sigma = 100$  S/m,  $\sigma = 50$  S/m and PEC.

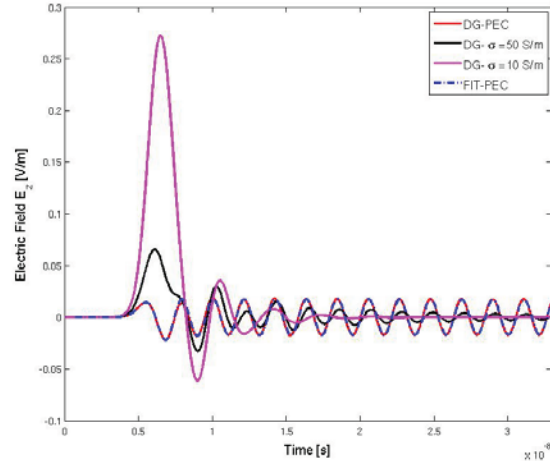


Fig. 7. Electric field in the center of the cavity.

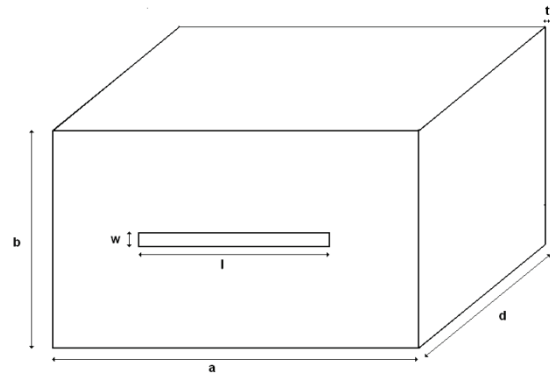


Fig. 8. 3D cavity.

A FFT is applied to the electric field, and the shielding effectiveness is plotted in Fig. 9. The result obtained with the PEC case (red) is similar to the analytical formulation (blue) [17]. For the case of finite conductivities, the shielding effectiveness is less important and the resonance peaks are attenuated due to the transmission of the shield.

In Fig. 10, the time domain electric fields are compared for the same cases. For the PEC case (black), the electric field is low, because it penetrates only by the aperture. For the other cases, the electric field remains important for low conductivities and decreases faster with time.

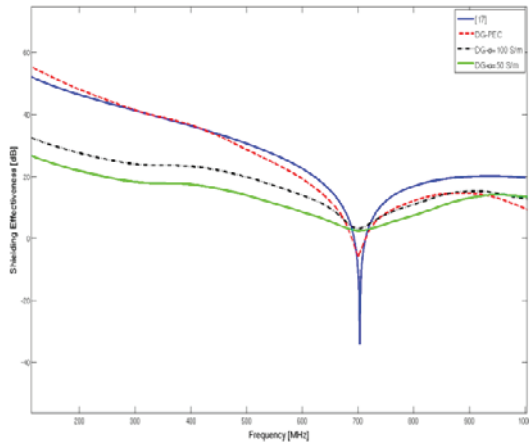


Fig. 9. Shielding effectiveness in the center of the cavity.

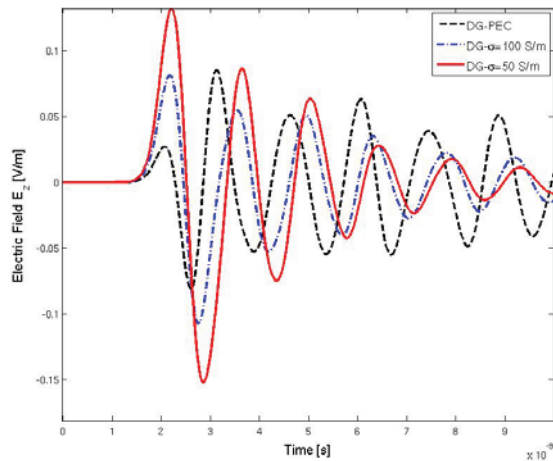


Fig. 10. Electric field in the center of the cavity.

## VII. CONCLUSION

An interface condition avoiding the mesh of thin resistive sheets is presented and allows a reduction of the computational cost when computing shielding effectiveness. It takes into account a sheet with a thickness smaller than the skin depth. The interface condition has been implemented in a 2D and 3D discontinuous Galerkin method, and has been validated for different scattering problems. The future developments will extend the interface condition for the case of dielectric composite material.

## REFERENCES

[1] K. Mitzner, "Effective boundary conditions for reflection and transmission by an absorbing shell of

arbitrary shape," *IEEE Trans. Antennas and Propag.*, vol. 16, no. 6, pp. 706-712, 1968.

- [2] R. Schulz, V. Plantz, and D. Brush, "Shielding theory and practice," *IEEE Trans. Electromagn. Comp.*, vol. 30, no. 3, pp. 187-201, 1988.
- [3] F. Bocquet, L. Pichon, A. Razek, and G. Tanneau, "3D FEM analysis of electromagnetic wave scattering from a dielectric sheet in EMC problems," *IEEE Trans. Magn.*, vol. 34, no. 5, pp. 2791-2794, 1998.
- [4] S. Van der Berghe, F. Olyslager, and D. De Zutter, "Accurate modeling of thin conducting layer in FDTD," *IEEE Microwave and Guided Wave Letters*, vol. 8, no. 2, pp. 75-77, 1998.
- [5] M. Sarto, "A new Model for the FDTD analysis of the shielding performances of thin composite structures," *IEEE Trans. Electromagnetic Comp.*, vol. 44, no. 4, pp. 298-306, 1999.
- [6] M. Feliziani, F. Maradei, and G. Tribellini, "Field analysis of penetrable conductive shields by the finite-difference time-domain method with impedance network boundary conditions (INBS's)," *IEEE Trans. Electromagnetic Comp.*, vol. 44, no. 4, pp. 307-319, 1999.
- [7] B. Cockburn, S. Hou, and C.-W. Shu, "TVB Runge-Kutta local projection discontinuous Galerkin finite element method for conservation laws IV: The multidimensional case," *Math. Comp.*, no. 54, pp. 545-581, 1990.
- [8] J. Hesthaven and T. Warburton, "Nodal high-order methods on unstructured grids: time domain solution of Maxwell's equations," *J. Comp. Phys.*, vol. 181, no. 1, pp. 186-221, 2002.
- [9] D. Gedney, C. Luo, J. Roden, R. Crawford, B. Guernsey, J. Miller, T. Kramer, and E. Lucas, "The discontinuous Galerkin finite-element time-domain method solution of Maxwell's equations," *ACES Journal*, vol. 24, no. 2, pp. 129-142, 2009.
- [10] V. Pr eault, R. Corcolle, L. Daniel, and L. Pichon, "Effective permittivity of shielding composite materials for microwave frequencies," *IEEE Trans. Electromagnetic Comp.* (accepted)
- [11] C. Holloway, M. Sarto, and M. Johansson, "Analyzing carbon-fiber composite materials with equivalent-layer models," *IEEE Trans. Electromagnetic Comp.*, vol. 47, no. 4, pp. 833-844, 2005.
- [12] L. Pebernet et al, "Discontinuous Galerkin method applied to electromagnetic compatibility: introduction of thin wire and thin resistive materials," *IET Sci. Meas. Technol.*, vol. 2, no. 6, pp. 395-401, 2001.
- [13] A. Kameni, A. Modave, M. Boubekur, V. Pr eault, L. Pichon, and C. Geuzaine, "Evaluation of shielding effectiveness of composite wall with a time domain discontinuous Galerkin method," *The*

*European Physical Journal - Applied Physics*.  
(accepted for publication)

- [14] L. Fezoui, S. Lanteri, S. Lohrengel, and S. Piperno, "Convergence and stability of a discontinuous Galerkin time-domain method for the 3D heterogeneous Maxwell's equations on unstructured meshes," *M2AN*, vol. 39, no. 6, pp. 1149-1176, 2005.
- [15] L. Bernard, R. Torrado, and L. Pichon, "Efficient implementation of UPML in generalized finite-difference time-domain method," *IEEE Trans. Magn.*, vol. 46, no. 8, pp. 3492-3495, 2010.
- [16] W. Abdelli, X. Mininger, L. Pichon, and H. Trabelsi, "Impact of composite materials on the shielding effectiveness of enclosures," *ACES Journal*, vol. 27, no. 4, pp. 369-375, 2012.
- [17] M. Robinson, T. Benson, C. Christopoulos, J. Dawson, M. Ganley, A. Marvin, S. Porter, and D. W. Thomas, "Analytical formulation for the shielding effectiveness of enclosures with apertures," *IEEE Trans. Electromagn. Compat.*, vol. 40, no. 3, pp. 240-248, 1998.



**Mohamed Boubekour** received his Master in Mathematical Modeling option Numerical analysis and PDE in Pierre et Marie Curie University, he is currently a PhD student at LGEP. His current research interests include electromagnetic compatibility shielding, Modeling of wave propagation for thin sheet.



**Abelin Kameni** is an Engineer from "Ecole D'Ingénieurs en Modélisation Mathématique et Mécanique (MATMECA)" in 2004. He received the Msc degree in Mathematical modeling from University of Bordeaux in 2005. In 2009 he earned a PhD in Electrical Engineering of Université Henri Poincaré from Nancy and joined the Laboratoire de Génie Electrique of Paris (LGEP) in 2010 as Assistant Professor. His research interests concern numerical methods applied to electromagnetic problems.



electromagnetic and mechanics.

**Axel Modave** is a physics engineer from the University of Liège in 2008. He is currently a PhD student in the Applied and Computational Electromagnetics group at the University of Liège. His research interests concern numerical methods for wave-like problems in



**Laurent Bernard** received the B.Sc. and M.Sc. degrees from the Institut National Polytechnique de Grenoble in 2004. In 2007, he received the Ph.D. from the Ecole Centrale de Lyon and the Universidade Federal de Minas Gerais (co-supervision). He is currently Research Engineer at the CNRS and works with the LGEP (Laboratoire de Génie Electrique de Paris). His research interests concern mesh-based numerical methods for electromagnetics and coupled problems.



**Lionel Pichon** is an Engineer from Ecole Supérieure d'Ingénieurs en Electronique et Electrotechnique (ESIEE) in 1984. In 1985 he joined the Laboratoire de Génie Electrique de Paris (LGEP) where he earned a PhD in electrical engineering in 1989. He got a position at the CNRS (Centre National de la Recherche Scientifique) in 1989. He is now Directeur de Recherche at the CNRS (Senior Scientist). Since 2002 he is one of the animators of the Groupement de Recherche CNRS, known as GDR Ondes, where is involved a large network of laboratories and researchers related to the modeling of wave propagation from mathematical theory to numerical solutions for particular applications.